Terr. Atmos. Ocean. Sci., Vol. 20, No. 2, 411-423, April 2009 doi: 10.3319/TAO.2008.01.09.01(Oc)

Comparative Geochemistry of ^{234}Th, ^{210}Pb, and ^{210}Po: A Case Study in the Hung-Tsai Trough off Southwestern Taiwan

Ching-Ling Wei*, Lin-Hwa Chou, Jing-Ru Tsai, Liang-Saw Wen, and Su-Cheng Pai

Institute of Oceanography, National Taiwan University, Taipei, Taiwan, ROC

Received 12 September 2007, accepted 9 January 2008

ABSTRACT

Detailed profiles of dissolved and particulate ^{234}Th, ^{210}Pb, and ^{210}Po activities at three stations in the Hung-Tsai Trough off southwestern Taiwan were determined. The total ^{234}Th activity is 20 ~ 25% deficient from its secular equilibrium in the entire water column. Except for an evident excess of ^{210}Po at some depths in the mixed layer and in the pycnocline layer, total ^{210}Po activity is also lower than total ^{210}Pb activity. As a result of atmospheric deposition, ^{210}Pb is about 25% in excess of its parent, ^{226}Ra, throughout the water column of the Hung-Tsai Trough. The ratios of the distribution coefficients of ^{234}Th, ^{210}Pb, and ^{210}Po show that the order of particle affinity is Po > Th ~ Pb in the mixed layer and bottom layer, whereas the order changes, due to particle regeneration, into Th > Pb > Po in the pycnocline layer of the Hung-Tsai Trough.

Mass balance equations incorporating horizontal advection are established to estimate the scavenging and removal rates of ^{234}Th, ^{210}Pb, and ^{210}Po. The vertical fluxes of ^{234}Th, ^{210}Pb, and ^{210}Po within the euphotic layer for the Hung-Tsai Trough are 6760, 630, and 400 dpm m^{-2} d^{-1}, respectively. The residence times of the three radionuclides in the euphotic zone are remarkably close to one another (within 2 weeks). By using ^{234}Th and ^{210}Po as proxies of particulate organic carbon and nitrogen, export flux from the euphotic layer of the Hung-Tsai is 40 mmol C m^{-2} d^{-1} based on the ^{234}Th approach and 64 mmol C m^{-2} d^{-1} based on the ^{210}Po approach.

Key words: Hung-Tsai Trough, ^{238}U-^{234}Th, ^{226}Ra-^{210}Pb, ^{210}Pb-^{210}Po, Export production

Citation: Wei, C. L., L. H. Chou, J. R. Tsai, L. S. Wen, and S. C. Pai, 2009: Comparative geochemistry of ^{234}Th, ^{210}Pb, and ^{210}Po: A case study in the Hung-Tsai Trough off southwestern Taiwan. Terr. Atmos. Ocean. Sci., 20, 411-423, doi: 10.3319/TAO.2008.01.09.01(Oc)

1. INTRODUCTION

The conveyance of particle-reactive elements from the upper water column to sediments significantly relies on the settling of particulate matter. The three most particle-reactive radionulides of ^{238}U-series, ^{234}Th, ^{210}Pb, and ^{210}Po have been extensively used as powerful tracers for the study of particle dynamics in the ocean. With a proper mass balance setup based on the fact that the radioactive disequilibrium between long-lived parent and short-lived daughter radionuclides reflects the vertical fluxes out of the system, export fluxes can then be quantitatively estimated.

Produced constantly from ^{238}U in seawater, ^{234}Th ($t_{1/2}$ = 24.1 d) is adsorbed quickly to particle surface and removed from the water column. The ^{238}U-^{234}Th disequilibrium has been widely used as a powerful tracer for particulate organic carbon and provides estimates of export production (see review of Buesseler et al. 2006). Although both ^{210}Po ($t_{1/2}$ = 138.4 days) and ^{210}Pb ($t_{1/2}$ = 22.2 yrs) are particle-reactive, the geochemical mechanisms that are responsible for their fate in marine environments are different. Previous measurements of ^{210}Po and ^{210}Pb in the ocean show that biological uptake may be more important than inorganic adsorption for ^{210}Po scavenging whereas ^{210}Pb tend to be adsorbed by inorganic particles.

There are very few previous studies that report ^{234}Th, ^{210}Pb, and ^{210}Po data determined from the same seawater sample. Tanaka and Tsunogai (1983) measured ^{234}Th, ^{210}Pb, and ^{210}Po activities in the same seawater samples and in settling particles collected from Funka Bay, Japan. Sarin et al. (1994) reported three vertical profiles of dissolved activities of ^{234}Th, ^{210}Pb, and ^{210}Po in the northeastern Arabian Sea. Harada and Tsunogai (1986) reported ^{234}Th, ^{210}Pb, and ^{210}Po activities in settling particles collected by sediment traps deployed in the Northeast Pacific and Antarctica. Wei and

* *Corresponding author*
E-mail: weic@ntu.edu.tw

Murray (1991, 1994) compared geochemical behavior of ^{234}Th, ^{210}Pb, and ^{210}Po in the Black Sea. Shimmield et al. (1995) simultaneously measured the three radionuclides from the same seawater samples collected in the upper 500 m in the marginal ice zone in Antarctica. Kim and Church (2001) presented dissolved and particulate ^{234}Th, ^{210}Pb, and ^{210}Po data simultaneously determined on the same samples collected from the Bermuda Time-series Stations (BATS). As part of JGOFS EqPac program, Murray et al. (2005) reported a complete ^{234}Th, ^{210}Pb, and ^{210}Po data set measured from the seawater samples collected in the upper water column and settling particles collected by floating traps in the Equatorial Pacific.

Off the southwestern tip of Taiwan, the Hung-Tsai Trough (Fig. 1) is a submarine canyon bathymetrically characterized by a narrow upper canyon with steep walls and a broad lower canyon with a flat floor (Yu and Chiang 1995). The Hung-Tsai Trough shows the hydrographic characteristics of the South China Sea (Fig. 2), which originated from the intrusion of Kuroshio Current through Bashi Channel (Shaw 1989). In the past few years, the region has been chosen as a training site for graduate students and has been visited regularly once or twice a year, so detailed oceanographic data, such as sb-ADCP, hydrographic and chemical parameters are available as auxiliary information to delineate geochemical processes.

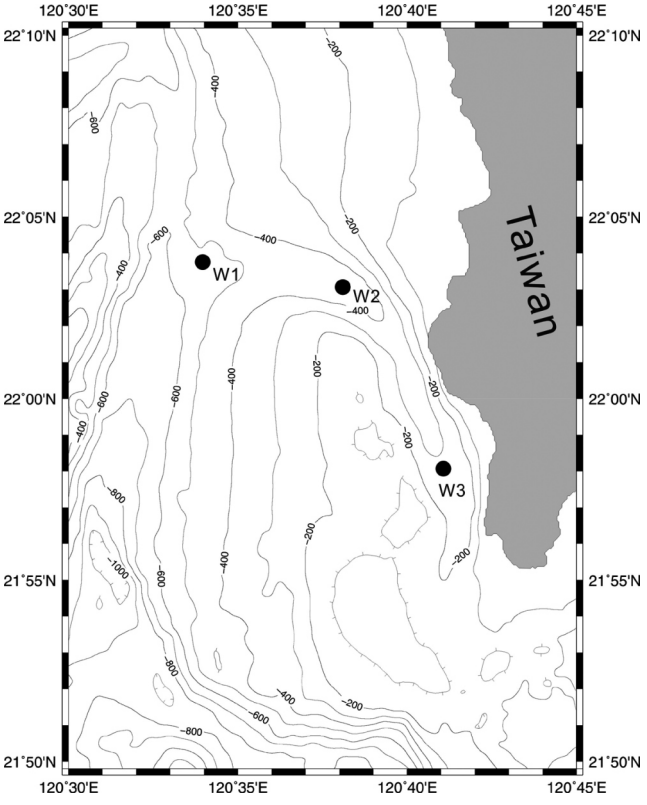

Fig. 1. Bathymetric map of the Hung-Tsai Trough and locations of sampling stations of OR1-784.

A detailed sampling of seawater for ^{234}Th, ^{210}Pb, and ^{210}Po determinations at three stations located along the axis of the Hung-Tsai Trough was carried out. The goals of this study are to use the collected data to (1) use the Hung-Tsai Trough as a test site to evaluate the feasibility of incorporating ADCP-derived current to the scavenging/removal model; (2) compare the geochemical behavior of ^{234}Th, ^{210}Pb, and ^{210}Po; and (3) to estimate the export flux of particulate organic carbon and nitrogen using ^{234}Th and ^{210}Po as proxies in the Hung-Tsai Trough.

2. MATERIALS AND METHODS

Seawater samples were collected at the three stations shown in Fig. 1 during 6 ~ 8 March 2006 (cruise #784), onboard R/V Ocean Researcher I. A CTD/20 L Go-Flo system was used to collect large volumes of seawater for ^{234}Th, ^{210}Pb, and ^{210}Po determinations. At each sampling depth, 40-L seawater was collected and divided into one 20-L and two 10-L subsamples. The 20-L sample was used to determine ^{234}Th and the two 10-L samples were used to determine ^{210}Pb and ^{210}Po, respectively. Seawater was immediately pressure-filtered by compressed air through a pre-weighed 142 mm Nuclepore filter (0.45 μm) mounted in a Plexiglas filter holder.

Filtered seawater was transferred into a cubitainer, acidified with approximately 20 ml of concentrated HCl and spiked with 35 dpm ^{230}Th yield tracer as well as 60 mg Fe carrier. Without interrupting the aeration, 12 N NaOH was added to raise the pH to 8. The $Fe(OH)_3$ precipitates, with

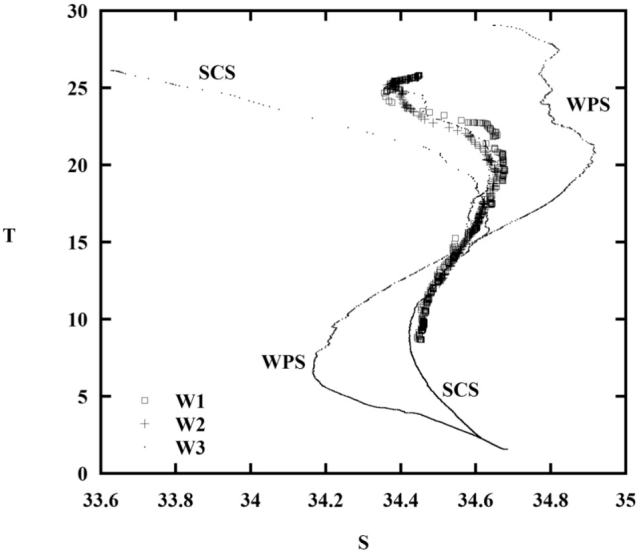

Fig. 2. T-S diagram of the three sampling stations in the Hung-Tsai Trough. Representative T-S curves of the South China Sea (SCS) and the West Philippine Sea (WPS) were taken from Station F of OR1-#575 (20 15'N, 118 39.6'E) and Station BV of OR1-#833 (20 24.48'N, 127 16.2'E), respectively.

adsorbed thorium, were collected by siphoning and centrifuging, and then dissolved in concentrated HCl to make the samples 9 N HCl. These samples were then passed through an anion exchange column (AG1X-8) preconditioned by 9N HCl to separate uranium from thorium. Thorium samples were purified by passing the sample through three anion exchange columns pre-conditioned with 8 N HNO_3. The sample was evaporated down to one drop and was ready for extraction. Th-234 and the yield tracer, ^{230}Th, were extracted into a 0.4 M TTA (thenoyltrifluoroacetone)-benzene solution and stippled on a stainless-steel disc. Preconcentration and separation of uranium and thorium from the filtered seawater samples were completed in three days after samples were collected.

The particulate samples collected on the Nuclepore filters were dried in a desiccator and weighed to estimate the concentration of total suspended matter. The filter was then decomposed and digested following the procedures of Anderson and Fleer (1982). In short, the filters were decomposed in the laboratory by soaking in ~10 ml of concentrated NH_4OH. The samples were gently heated to evaporate the NH_4OH then fluxed in $HClO_4$/HF to thoroughly digest organic and inorganic materials. After digestion, the samples were purified and mounted on stainless-steel discs following the same procedures as for dissolved ^{234}Th samples.

The activities of ^{234}Th were counted by a low background (< 0.15 cpm) anticoincidence counter (Riso GM25-5) via its -emitting daughter ^{234}Pa. Chemical yield of thorium was estimated by counting spiked ^{230}Th using silicon surface-barrier detectors (EG&G Ortec 576). The counting efficiencies of the detectors were calibrated against NIST traceable ^{230}Th (Isotope Products Laboratory 387-67-3) standard plates. Activities of ^{234}Th reported here were corrected back to the sampling time after the ingrowth of ^{234}Th from ^{238}U was subtracted.

The filtrate from the ^{210}Po sample was acidified with about 10 ml concentrated HCl and spiked with 2.2 dpm of ^{209}Po and 30 mg of Fe carrier. Given 2 days isotopic equilibration time, concentrated NH_4OH was then added to raise the pH~8 to precipitate $Fe(OH)_3$. The $Fe(OH)_3$ precipitate was collected by decanting and centrifuging and dissolved in HCl, digested with HNO_3, and ^{210}Po and ^{209}Po were spontaneously plated onto silver plates following Flynn (1968). The particulate samples collected on the Nuclepore filters were dried in a desiccator and weighed to estimate the concentration of total suspended matter. The filter was than decomposed and digested following the procedures of Anderson and Fleer (1982). The same procedures as for dissolved samples were carried out to plate ^{210}Po and ^{209}Po onto silver plates.

The 10-L seawater samples for ^{210}Pb determination were stored for at least 1 year to let ^{210}Po grow in from ^{210}Pb; then the same procedures for dissolved and particulate ^{210}Po were followed. The silver discs were counted by alpha spectrometry (EG&G Ortec 576).

Collected by separate hydrocasts, about 5 L of seawater for particulate organic carbon and total nitrogen was filtered through a pre-combusted (450 C) Whatman 25 mm GF/F filter, wrapped in aluminum foil and stored at -4 C. In the laboratory, the filter was acid-fumed to remove carbonates and then wrapped firmly into tin boats and loaded into the autosampler of Fisons elemental analyzer (NA1500). Calibration curve was obtained by running acetanilide (C_8H_9NO) standard. The overall procedural errors estimated from duplicates are better than 2% for both carbon and nitrogen determinations.

3. RESULTS AND DISCUSSION

Table 1 gives depth, ^{238}U activities calculated from Ku et al. (1977), concentrations of total suspended matter measured from subsamples for ^{234}Th (TSM_{Th}), ^{210}Pb (TSM_{Pb}), and ^{210}Po (TSM_{Po}), dissolved and particulate ^{234}Th (DTh and PTh), ^{210}Pb (DPb and PPb), and ^{210}Po (DPo and PPo) activities, and concentrations of particulate organic carbon (POC) and particulate nitrogen (PN) at the three sampling stations in the Hung-Tsai Trough. Uncertainties of all radioisotope data listed were estimated according to the propagation of counting error (1). Note: hydrographic and nutrients data are not listed but are available upon request.

3.1 Hydrography and Vertical Distributions of ^{234}Th, ^{210}Pb, and ^{210}Po

Measured by PAR sensor attached to CTD/Rosette system, the euphotic depth at all three stations was 80 m. The T-S diagram of the three stations is shown in Fig. 2, in which the typical T-S curves of the South China Sea (SCS) and the Western Philippine Sea (WPS) were also shown. Representative T-S curves of the SCS and the WPS were taken from Station F of OR1-#575 (20 15'N, 118 39.6'E) and Station BV of OR1-#833 (20 24.48'N, 127 16.2'E), respectively. It can be seen that the hydrographic characteristics of the study area is similar to that of the water in the South China Sea . The vertical profiles of potential density at the three sampling stations are shown in Fig. 3. The pycnocline layer, in the depth range of 50 to 200 m, shoals from the lower canyon to the upper canyon. The pronounced oscillation of the pycnocline as a result of semi-diurnal tide in the region has been observed (Liang et al. 1985).

Composite vertical profiles of the dissolved and particulate activities of the three radionuclides at the three sampling stations are shown in Fig. 4. It can be seen that the data shows as being somewhat scattering. The degree of scatterings was significantly reduced if the activities were plotted against density (Fig. 5), indicating the effect of vertical movement of water through the sampling period caused by tidal forcing. Consequently, in order to minimize

Table 1. Depth, calculated ^{238}U activities from Ku et al. (1977), concentrations of total suspended matter measured from subsamples for ^{234}Th (TSM_{Th}), ^{210}Pb (TSM_{Pb}), and ^{210}Po (TSM_{Po}), dissolved, particulate ^{234}Th (DTh and PTh), ^{210}Pb (DPb and PPb), and ^{210}Po (DPo and PPo) activities, and concentrations of particulate organic carbon (POC) and particulate nitrogen (PN) at three sampling stations in the Hung-Tsai Trough.

Station	Depth	^{238}U	TSM_{Th}	TSM_{Pb}	TSM_{Po}	DTh	PTh	DPb	PPb	DPo	PPo	POC	PN
	m	dpm L^{-1}		mg L^{-1}		dpm L^{-1}	dpm L^{-1}	dpm $100L^{-1}$	dpm $100L^{-1}$	dpm $100L^{-1}$	dpm $100L^{-1}$	μM	
W1	0	2.44	0.51	0.42	0.91	-	0.059 ± 0.005	12.97 ± 0.77	0.63 ± 0.20	8.95 ± 0.57	2.57 ± 0.36	-	-
22°03.76'N	5	2.44	0.26	0.51	0.64	1.735 ± 0.043	0.209 ± 0.010	12.89 ± 0.76	0.94 ± 0.22	5.33 ± 0.53	2.96 ± 0.37	-	-
120°33.96'E	10	2.44	0.28	0.46	0.76	1.514 ± 0.035	0.264 ± 0.010	12.29 ± 0.78	1.12 ± 0.23	6.28 ± 0.43	2.34 ± 0.30	4.31	0.53
	20	2.44	0.20	1.18	0.69	2.201 ± 0.081	0.156 ± 0.007	12.80 ± 0.81	2.00 ± 0.30	4.84 ± 0.49	2.48 ± 0.32	4.53	0.64
	40	2.44	0.29	0.67	0.81	2.147 ± 0.064	0.452 ± 0.039	9.64 ± 0.69	1.75 ± 0.29	11.77 ± 0.85	2.99 ± 0.43	4.81	0.72
	60	2.44	0.53	0.72	0.83	1.650 ± 0.069	0.395 ± 0.018	10.10 ± 0.71	2.80 ± 0.37	6.61 ± 0.58	2.84 ± 0.38	3.61	0.53
	80	2.43	0.68	0.95	1.11	0.896 ± 0.035	0.662 ± 0.031	6.93 ± 0.51	3.37 ± 0.37	6.20 ± 0.43	2.26 ± 0.34	-	-
	100	2.43	0.98	0.96	0.97	0.596 ± 0.018	0.946 ± 0.034	6.07 ± 0.44	3.57 ± 0.36	4.49 ± 0.49	2.54 ± 0.38	3.35	0.44
	200	2.45	0.42	0.31	0.47	1.343 ± 0.026	0.420 ± 0.020	11.72 ± 0.60	3.00 ± 0.30	4.52 ± 0.52	1.94 ± 0.29	1.27	0.12
	300	2.44	0.26	0.83	0.54	1.317 ± 0.029	0.412 ± 0.026	10.07 ± 0.63	2.21 ± 0.28	2.83 ± 0.41	2.23 ± 0.32	1.30	0.13
	400	2.44	0.36	0.44	0.87	1.388 ± 0.048	0.451 ± 0.021	17.72 ± 0.90	1.77 ± 0.27	6.03 ± 0.59	2.21 ± 0.39	4.72	0.63
W2	0	2.44	0.27	0.52	0.93	2.154 ± 0.062	0.254 ± 0.016	11.46 ± 0.69	1.15 ± 0.19	5.88 ± 0.54	3.05 ± 0.37	9.50	1.28
22°03.07'N	5	2.44	0.29	0.00	0.00	2.157 ± 0.066	0.199 ± 0.012	-	-	-	-	4.88	0.71
120°38.10'E	10	2.44	0.25	0.73	0.64	2.535 ± 0.081	0.236 ± 0.021	11.71 ± 0.77	1.26 ± 0.27	8.00 ± 0.53	3.71 ± 0.43	4.59	0.67
	20	2.44	0.29	0.46	0.36	2.163 ± 0.055	0.250 ± 0.015	13.05 ± 0.73	1.30 ± 0.25	5.48 ± 0.28	2.20 ± 0.32	5.04	0.72
	40	2.43	0.85	0.65	0.64	1.754 ± 0.067	0.679 ± 0.033	9.39 ± 0.50	2.02 ± 0.29	4.99 ± 0.47	2.38 ± 0.34	4.27	0.59

Table 1. (Continued)

Station	Depth	^{238}U	TSM_{Th}	TSM_{Pb}	TSM_{Po}	DTh	PTh	DPb	PPb	DPo	PPo	POC	PN
	m	dpm L^{-1}		mg L^{-1}		dpm L^{-1}	dpm L^{-1}	dpm 100L^{-1}	dpm 100L^{-1}	dpm 100L^{-1}	dpm 100L^{-1}	μM	
	60	2.43	1.04	0.76	0.98	0.761 ± 0.021	0.376 ± 0.022	7.70 ± 0.48	3.48 ± 0.40	4.78 ± 0.20	1.83 ± 0.27	4.14	0.60
	80	2.44	0.56	1.14	1.22	0.945 ± 0.022	0.590 ± 0.033	10.19 ± 0.65	3.13 ± 0.36	3.41 ± 0.31	2.06 ± 0.33	3.73	0.54
	100	2.44	0.45	0.49	0.57	1.419 ± 0.038	0.379 ± 0.021	9.89 ± 0.65	2.07 ± 0.25	3.92 ± 0.25	1.67 ± 0.28	2.62	0.35
	150	2.45	0.27	0.51	0.46	1.778 ± 0.058	0.328 ± 0.019	8.94 ± 0.67	1.97 ± 0.27	9.87 ± 0.73	1.33 ± 0.25	1.72	0.25
	200	2.45	0.32	0.49	0.22	1.113 ± 0.046	0.477 ± 0.029	9.60 ± 0.71	3.12 ± 0.27	6.70 ± 0.62	1.59 ± 0.26	1.48	0.15
	300	2.45	0.45	0.34	0.54	1.306 ± 0.041	0.272 ± 0.017	7.17 ± 0.57	2.38 ± 0.30	7.80 ± 0.51	1.46 ± 0.26	2.53	0.20
W3	0	2.44	0.42	0.58	1.21	1.288 ± 0.051	0.438 ± 0.021	11.34 ± 0.71	2.09 ± 0.31	3.77 ± 0.42	3.82 ± 0.47	8.20	1.12
21°58.07'N	5	2.44	0.27	0.55	0.67	2.378 ± 0.068	0.197 ± 0.016	7.25 ± 0.60	2.70 ± 0.32	9.39 ± 0.69	1.92 ± 0.31	4.13	0.69
120°41.07'E	10	2.44	0.26	0.58	0.63	1.393 ± 0.030	0.298 ± 0.016	10.04 ± 0.70	1.67 ± 0.26	7.53 ± 0.60	2.31 ± 0.34	1.96	0.30
	20	2.44	0.42	0.81	0.75	1.434 ± 0.050	0.753 ± 0.034	9.08 ± 0.51	3.20 ± 0.38	3.87 ± 0.48	2.56 ± 0.31	3.94	0.60
	40	2.44	0.42	0.80	0.89	0.959 ± 0.025	0.746 ± 0.039	5.31 ± 0.46	3.12 ± 0.35	8.03 ± 0.53	2.34 ± 0.35	3.79	0.40
	60	2.44	0.48	0.65	0.78	1.272 ± 0.034	0.598 ± 0.023	7.76 ± 0.61	2.89 ± 0.35	4.64 ± 0.59	2.06 ± 0.40	2.35	0.32
	80	2.45	0.27	0.42	0.71	1.343 ± 0.040	0.820 ± 0.027	9.74 ± 0.71	2.49 ± 0.34	11.18 ± 0.76	1.24 ± 0.24	2.16	0.32
	100	2.45	0.45	0.47	0.44	1.542 ± 0.049	0.525 ± 0.033	7.45 ± 0.73	1.50 ± 0.24	10.42 ± 0.75	1.68 ± 0.29	1.12	0.12
	150	2.45	0.34	0.65	1.04	1.947 ± 0.066	0.382 ± 0.019	6.57 ± 0.53	2.36 ± 0.27	14.61 ± 0.92	2.34 ± 0.38	1.82	0.19
	200	2.45	0.33	0.95	0.46	2.170 ± 0.058	0.406 ± 0.028	10.36 ± 0.72	4.07 ± 0.40	8.17 ± 0.61	2.47 ± 0.33	2.21	0.19
	250	2.44	0.50	0.54	0.72	-	0.425 ± 0.023	8.93 ± 0.66	2.78 ± 0.36	4.17 ± 0.48	2.02 ± 0.27	1.26	0.12

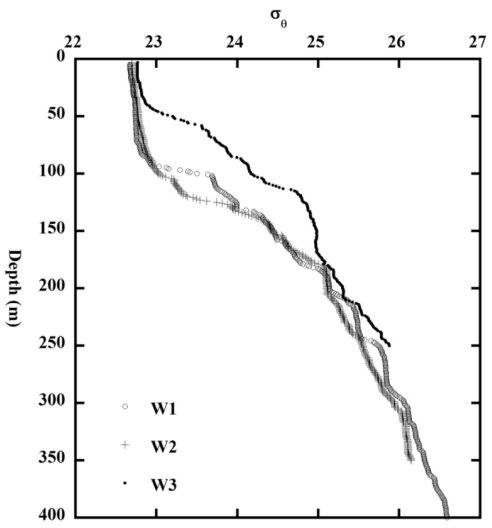

Fig. 3. Vertical profiles of potential density at the three sampling stations.

the variability caused by oscillation of the water body, the plots of parameters versus potential density instead of depth will preferably be used for later discussion.

3.2 ^{238}U-^{234}Th, ^{226}Ra-^{210}Pb, and ^{210}Pb-^{210}Po Disequilibria

The activity ratios of total ^{234}Th to ^{238}U (TTh/U), total ^{210}Pb to ^{226}Ra (TPb/Ra), and total ^{210}Po to total ^{210}Pb (TPo/TPb) are shown in Fig. 6. Apart from a few depths in the mixed layer, total ^{234}Th activity was 10 ~ 40% deficient or 20 to 25% for the whole water column, from its secular equilibrium in the entire water column of the Hung-Tsai Trough. Similar to the previous results obtained in the vicinity (Hung and Wei 1992; Wei et al. 1994) the ^{234}Th activity is essentially deficient relative to ^{238}U throughout the whole water column, indicating dynamic scavenging phenomenon in the region.

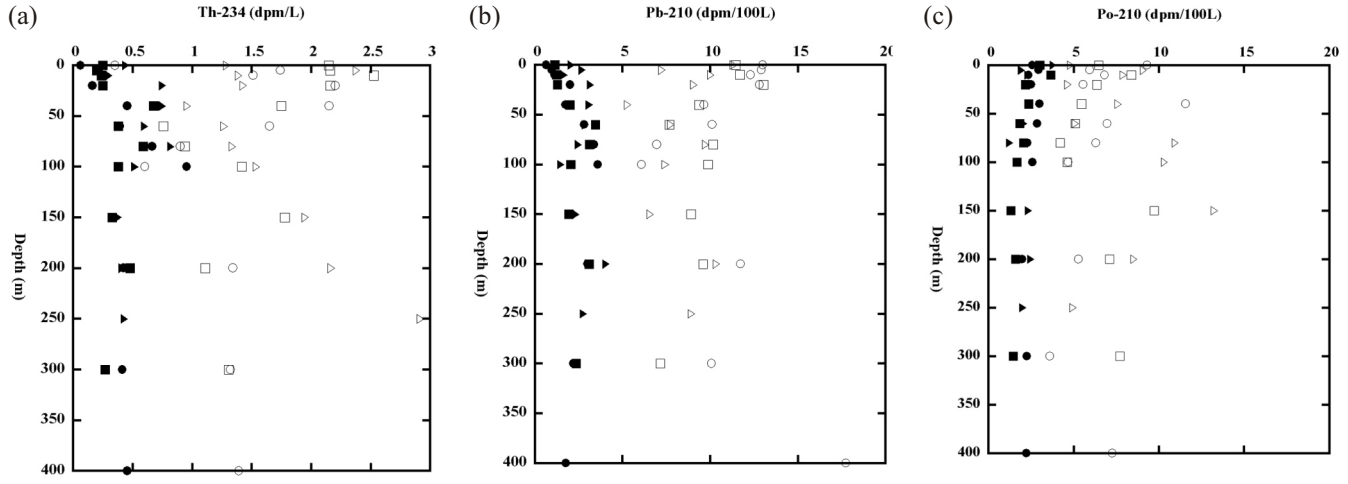

Fig. 4. Composite vertical profiles of the dissolved (open symbols) and particulate (filled symbols) (a) ^{234}Th, (b) ^{210}Pb, and (c) ^{210}Po at sampling station W1 (circles), W2 (squares), and W3 (triangles).

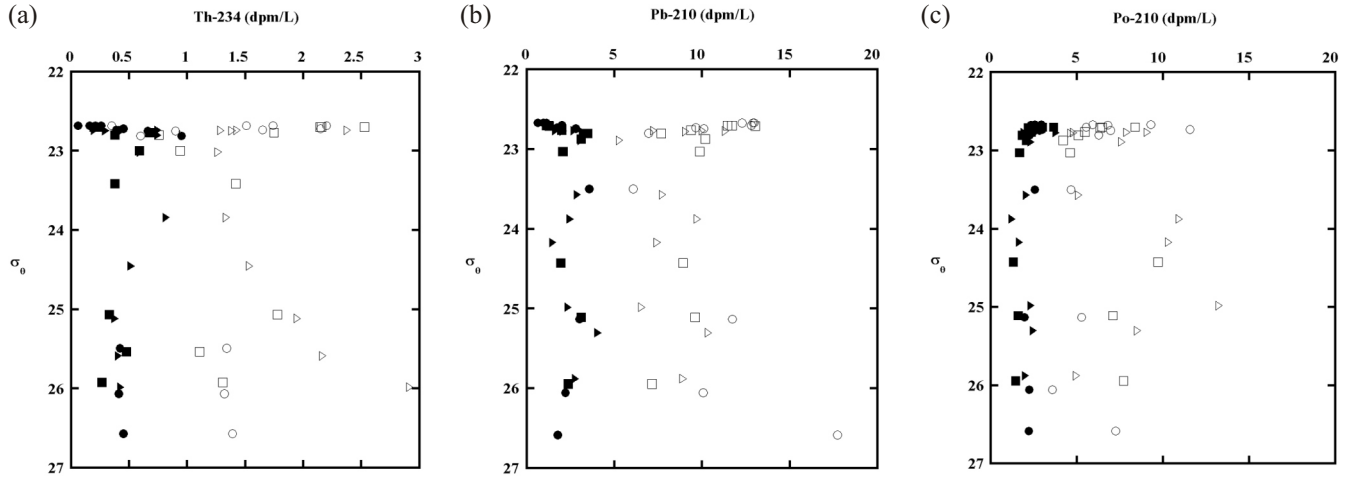

Fig. 5. -activity plots of the dissolved (open symbols) and particulate (filled symbols) (a) ^{234}Th, (b) ^{210}Pb, and (c) ^{210}Po at sampling station W1 (circles), W2 (squares), and W3 (triangles).

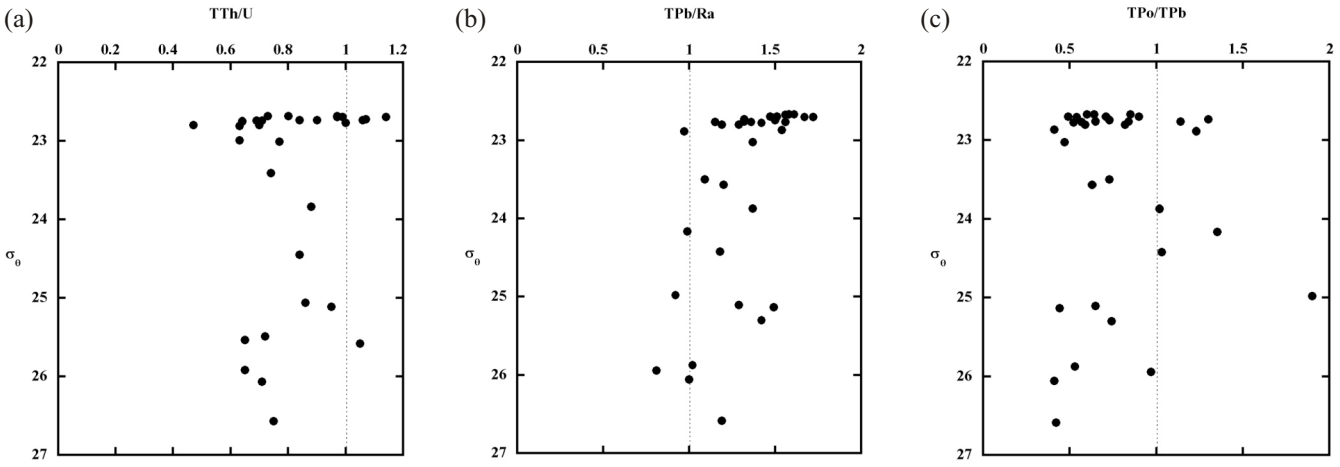

Fig. 6. -activity ratios of (a) total ^{234}Th to ^{238}U, (b) total ^{210}Pb to ^{226}Ra, and (c) total ^{210}Po to ^{210}Pb at the three sampling stations. Dashed lines represent secular equilibrium of parent-daughter pair.

Essentially, ^{210}Pb activity is higher than its parent throughout the whole water column (Fig. 6b). Standing stock of excess ^{210}Pb in the water column of the HungTsai Trough increases toward the lower canyon, from 0.35 dpm cm^{-2} at the shallowest W3 to 1.03 dpm cm^{-2} at the deepest W1. This excess ^{210}Pb is much lower than the values found in the Okinawa Trough (~10 dpm cm^{-2}, Nozaki et al. 1990) and comparable with the Equatorial Pacific Ocean (0.1 ~ 1.6 dpm cm^{-2}, Murray et al. 2005). Since the excess ^{210}Pb signal was still observed at our deepest sampling depth, this value represents the minimum residual amount of deposited ^{210}Pb from the atmosphere after particle removal and physical transport. Considering the closeness of the continental source of ^{222}Rn at the site, the low excess ^{210}Pb in the Hung-Tsai Trough implies a very fast removal rate.

Polonium removal from the ocean is tightly related to biological activity as supported by the correlations of ^{210}Po deficiency relative to ^{210}Pb with POC concentration (Sarin et al. 1999) and the removal rate constant with chlorophyll concentration (Nozaki et al. 1998). The deviation of TPo from secular equilibrium was relatively larger (lowest TPo/TPb activitiy ratio as low as 0.3) in the surface layer and in the bottom layer (Fig. 6c). However, an evident excess of ^{210}Po was observed at some depths in the mixed layer and in the layer of = 24 ~ 25. An excess of ^{210}Po (TPo/TPb > 1) below the mixed layer was commonly observed in the productive oceans (Bacon et al. 1988; Sarin et al. 1994). Chung and Wu (2005) reported vertical profiles of dissolved and particulate ^{210}Pb and ^{210}Po at three stations in the northern Luzon Strait. Although only 74 km to the southwest of our study area, excess ^{210}Po was not observed in the Luzon Enter Strait, which may be a result of different water masses between the two study sites.

The comparisons of the ratios of ^{210}Po and ^{210}Pb in the dissolved (DPo/DPb) and particulate (PPo/PPb) phases provide some insight into the fractionation of the two radionuclides (Fig. 7). Except at some depths in the euphotic zone and in the intermediate layer, the DPo/DPb ratio is lower than unity (Fig. 7a) and shows similar distribution with TPo/TPb (Fig. 6c). For those layers with excess DPo relative to DPb, polonium is released back to seawater due to particle regeneration, which is commonly observed in different oceanic regimes (Bacon et al. 1976; Murray et al. 2005). It should be noted that settling particles may be entrained and the enhancement of the particle decomposition may occur due to longer residence time in the pycnocline of = 23.5 ~ 25.5. Unlike the distribution of DPo/DPb ratio, the PPo/PPb ratios (Fig. 7b) are larger than unity (the highest value is 4) only in the surface layer, indicating preferential uptake of ^{210}Po by planktons residing in the surface water of the Hung-Tsai Trough. The enrichment of Po in the suspended particles corroborate the findings of Sarin et al. (1999), who found significant correlation between ^{210}Po deficiency relative to ^{210}Pb with POC concentration in the upper 500 m of the South Atlantic.

3.3 Partitioning of ^{234}Th, ^{210}Pb, and ^{210}Po

The partitioning of one element between dissolved and particulate phases reflects the reactivity of the element to particle surfaces. Conventionally, the distribution coefficient, K_d, has been used as an index of the degree of reactivity. The distribution coefficients of the radionuclides are calculated as

$$K_d = \frac{A_{part}}{A_{diss}} \frac{1}{TSM} \times 10^6 \quad (1)$$

where A_{Diss} and A_{Part} are dissolved and particulate activities, respectively, of the radionuclides of interest. Unlike

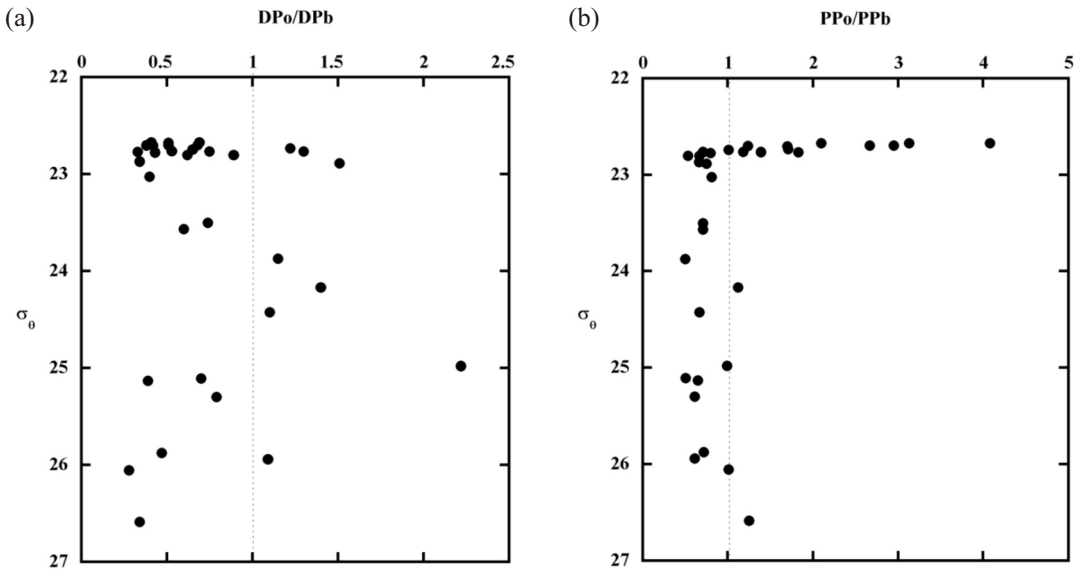

Fig. 7. -activity ratios of (a) dissolved ^{210}Po to dissolved ^{210}Pb and (b) particulate ^{210}Po to particulate ^{210}Pb at the three sampling stations. Dashed lines represent secular equilibrium.

the observation of the negative K_d-TSM correlations from many studies (e.g., Honeyman et al. 1988; Wei and Murray 1994), the K_d-TSM correlations of ^{234}Th, ^{210}Pb, and ^{210}Po obtained from the Hung-Tsai Trough are not as obvious because of the narrow range of TSM concentration. However, as shown in Fig. 8, the K_d of ^{234}Th [K_d(Th)] and ^{210}Pb [K_d(Pb)] correlate with the organic fraction of suspended particles, whereas the correlation is not as significant for ^{210}Po [K_d(Po)]. The result implies that, in addition to the particle concentration effect (Honeyman et al. 1988), the composition of particulate matter also plays an important role in the partitioning of the radionuclides.

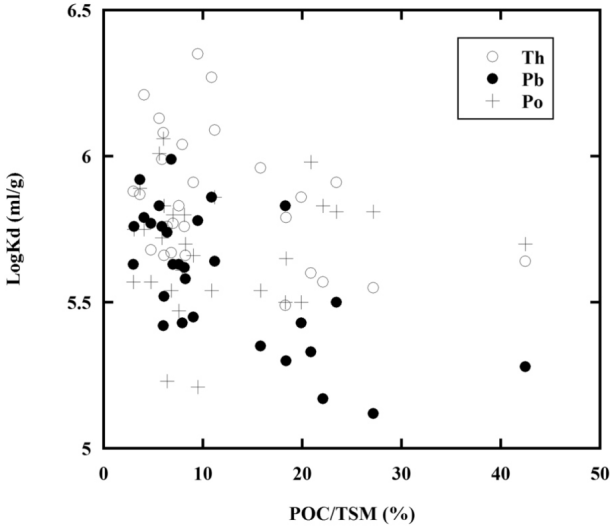

Fig. 8. Correlation of distribution coefficient of ^{234}Th (open circles), ^{210}Pb (filled circles), and ^{210}Po (crosses) and organic fraction of total suspended matter.

To compare the geochemical behavior of ^{234}Th, ^{210}Pb, and ^{210}Po, the fractionation factor, which is the ratio of the K_ds of the radionuclide of interest, is calculated. Plotting against density, vertical distributions of the ratio of K_ds of the three radionuclides are shown in Fig. 9. It can be seen that three distinctive layers of the Hung-Tsai Trough can be identified. In the mixed layer where the suspended particles are enriched in organic materials (POC/TSM > 10%, Fig. 9a), K_d(Po) shows the highest values among the three radionuclides (Figs. 9c, d), which is consistent with the common view that polonium is preferentially scavenged by biogenic particles (Shannon et al. 1970). In the pycnocline layer (= 23 ~ 25), K_d(Th) tends to exceed K_d(Pb) and K_d(Po) to show the fractionation factor < 1 (Figs. 9b, c), as a result of the particle regeneration process when settling down from the euphotic layer (Bacon et al. 1988). Though not as evident as in the mixed layer, K_d(Po) also seems higher than K_d(Pb) and K_d(Th) in the bottom layer of the Hung-Tsai Trough. Considering the relative shallow water column (300 ~ 500 m) of the Hung-Tsai Trough, it is possible that the particles in the bottom layer are residual particles that survived decomposition during descent from the surface and are still enriched in organic content thereby raising the K_d(Po).

3.4 Scavenging and Removal Rates of ^{234}Th, ^{210}Pb, and ^{210}Po

For budgeting ^{234}Th in the Hung-Tsai Trough, two equations, one for dissolved and one for particulate ^{234}Th, are established as follows.

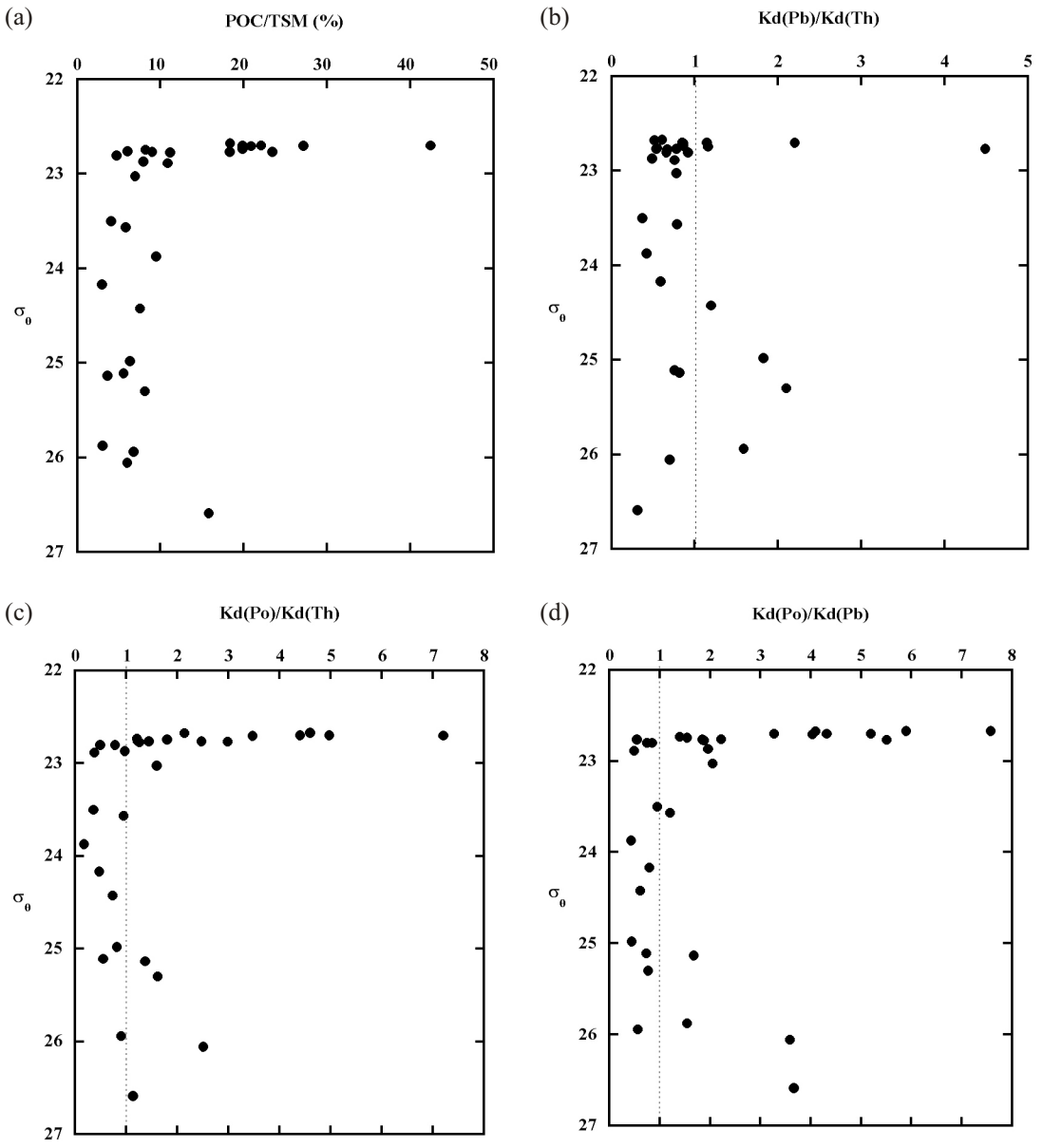

Fig. 9. (a) versus organic fraction of suspended matter, (b) -fractionation factors of ^{210}Pb and ^{234}Th, (c) ^{210}Po to ^{234}Th, and (d) ^{210}Po to ^{210}Pb at the three sampling stations.

$$\frac{\partial DTh_{W2}}{\partial t} = \frac{V_{W2}(DTh_{W1} - DTh_{W3})}{\Delta L} + \lambda_{Th} U_{W2} - \lambda_{Th} DTh_{W2} - J_{Th} \quad (2)$$

$$\frac{\partial PTh_{W2}}{\partial t} = J_{Th} + \frac{V_{W2}(PTh_{W1} - PTh_{W3})}{\Delta L} - \lambda_{Th} PTh_{W2} - R_{Th} \quad (3)$$

where

U_{W2} = average ^{238}U activity in the mixed layer of station W2 (dpm m^{-3});

DTh_i = dissolved ^{234}Th activity in the mixed layer of station i (dpm m^{-3});

PTh_i = particulate ^{234}Th activity in the mixed layer of station i (dpm m^{-3});

V_{W2} = average current velocity in the mixed layer of station W2 (m d^{-1});

L = distance between stations W1 and W3 (28700 m);

$_{Th}$ = radioactive decay constant of ^{234}Th (d^{-1});

J_{Th} = net scavenging rate of dissolved ^{234}Th in the mixed layer of station W2 (dpm m^{-3} d^{-1});

R_{Th} = net removal rate of particulate ^{234}Th in the mixed layer of station W2 (dpm m^{-3} d^{-1}).

The residence times of dissolved ($_{DTh}$) and particulate ($_{PTh}$) ^{234}Th relative to scavenging and removal rates, respectively,

can be calculated by the quotients of activities and changing rates.

$$\tau_{DTh} = \frac{DTh}{J_{Th}} \quad (4)$$

$$\tau_{PTh} = \frac{PTh}{R_{Th}} \quad (5)$$

The mass balance equations for ^{210}Po data are shown below and it can be seen that the equations are very similar to that for ^{234}Th except additional source for particulate ^{210}Po from adsorbed ^{210}Pb.

$$\frac{\partial DPo_{W2}}{\partial t} = \frac{V_{W2}(DPo_{W1} - DPo_{W3})}{\Delta L} + \lambda_{Po} DPb_{W2} - \lambda_{Po} DPo_{W2} - J_{Po} \quad (6)$$

$$\frac{\partial PPo_{W2}}{\partial t} = J_{Po} + \frac{V_{W2}(PPo_{W1} - PPo_{W3})}{\Delta L} + \lambda_{Po}(PPb_{W2} - PPo_{W2}) - R_{Po} \quad (7)$$

The residence times of dissolved ($_{DPo}$) and particulate ($_{PPo}$) ^{210}Po can be calculated.

$$\tau_{DPo} = \frac{DPo}{J_{Po}} \quad (8)$$

$$\tau_{PPo} = \frac{PPo}{R_{Po}} \quad (9)$$

With the replacement of subscripts to indicate values for ^{210}Po, the definitions for the parameters, variables, and constants in Eqs. (6) - (9) are the same as those for ^{234}Th.

As for ^{210}Pb, somewhat different consideration is given due to the fact that, in addition to the radioactive decay from ^{226}Ra, the major source of ^{210}Pb in the surface ocean is atmospheric deposition. Since there is no evidence regarding the phase of atmospheric ^{210}Pb deposition into the ocean, only total ^{210}Pb (TPb = DPb + PPb) is considered to establish the equation.

$$\frac{\partial TPb_{W2}}{\partial t} = \frac{I_{Pb}}{400} + \frac{V_{W2}(TPb_{W1} - TPb_{W3})}{\Delta L} + \lambda_{Pb}(Ra_{W2} - TPb_{W2}) - R_{Pb} \quad (10)$$

where

I_{Pb} = atmospheric ^{210}Pb flux in dpm m^{-2} d^{-1};

TPb_i = total ^{210}Pb activity in the mixed layer of station i (dpm m^{-3});

Ra_i = ^{226}Ra activity in the mixed layer of station i (dpm m^{-3});

$_{Pb}$ = radioactive decay constant of ^{210}Pb (1 d^{-1});

R_{Pb} = net removal rate of ^{210}Pb in the mixed layer of station W2 (dpm m^{-3} d^{-1}).

Ra-226 activities were not measured in this study. Correlation equation derived from ^{226}Ra activities and SiO_2 concentrations of the equatorial Pacific (Ku et al. 1995), the North Pacific (Nozaki et al. 1990), and the South China Sea (Nozaki and Yamamoto 2001), ^{226}Ra (dpm 100 L^{-1}) = 8.06 + 0.124 SiO_2 (M), was used to estimate ^{226}Ra activities in the Hung-Tsai Trough. The atmospheric ^{210}Pb flux in the study region was assumed to be 2 dpm cm^{-2} yr^{-1} or 54 dpm m^{-2} d^{-1} (Yang 2001).

The residence time of total ^{210}Pb ($_{Pb}$) is calculated by:

$$\tau_{Pb} = \frac{TPb}{R_{Pb}} \quad (11)$$

To evaluate the significance of temporal change of the activities of the radionuclides, we use the two data sets (unpublished results) collected from the two cruises to station W1 of this study. The two cruises, OR1-#742 (24 ~ 26 December 2004) and OR1-#744 (3 ~ 6 March 2005), were separated by 70 days. The temporal changing rates were 6, 0.08, and 0.2 dpm m^{-3} d^{-1} for ^{234}Th, ^{210}Pb, and ^{210}Po, respectively. The temporal change of the radionuclide activities was generally less than 10% of the radioactive decay rate of each radionuclide. Hence, it is acceptable to assume the steady-state condition ($\frac{Th}{t}$ $\frac{Po}{t}$ $\frac{Pb}{t}$ 0) for the distribution of these radionuclides in the Hung-Tsai Trough.

As pointed out by Savoye et al. (2006), the most difficult task of accurately estimating the physical transport of ^{234}Th in the scavenging/removal model is the availability of mean current velocity in the study region. Here we attempt to apply the average current derived from the historical shipboard ADCP data measured in the study area. Following the procedures of Liang et al. (2003), mean current velocity in the Hung-Tsai Trough was estimated by averaging archived shipboard ADCP data (NCOR Data Bank) collected in March during 1991 ~ 2006. The average current in the upper 100 m is 12.4 cm s^{-1} with a general direction along the axis of the trough, in agreement with the measurement by moored current meter (Liang et al. 1985).

The average radionuclide activity at the three sampling stations and the results of the scavenging model are shown in Table 2. In the table, for the purpose of comparison, various changing rates and residence times calculated from the scavenging model without horizontal transport are listed in italics. Average activity was calculated by dividing the radionuclide inventories in the euphotic layer by 80 m, the euphotic depth measured by the PAR sensor.

The vertical ^{234}Th flux, 6760 dpm m^{-2} d^{-1}, can be calculated by multiplying the removal rate, R_{Th}, by the euphotic depth. At the site, about 55 km to the northwest of the Hung-Tsai Trough, vertical ^{234}Th fluxes ranging from 363 to 2290 dpm m^{-2} d^{-1} in the upper 450 m were measured by sediment traps (Wei et al. 1994). It is not unreasonable that

Table 2. Average activities of dissolved and particulate ^{234}Th, ^{210}Pb, and ^{210}Po in the euphotic layer at three sampling stations and results of scavenging model of the Hung-Tsai Trough.

	Average activity (dpm m^{-3})					
Station	**DTh**	**PTh**	**DPb**	**PPb**	**DPo**	**PPo**
W1	1778	364	106	21	75	27
W2	1592	427	94	22	48	22
W3	1314	634	79	28	67	22

	V = 12.4 cm s^{-1}	V = 0 cm s^{-1}
J_{Th} (dpm m^{-3} d^{-1})	197.7	24.3
J_{Po} (dpm m^{-3} d^{-1})	3.1	0.2
R_{Th} (dpm m^{-3} d^{-1})	84.5	12.0
R_{Po} (dpm m^{-3} d^{-1})	5.0	0.2
R_{Pb} (dpm m^{-3} d^{-1})	7.9	0.7
τ_{DTh} (day)	8.0	66.0
τ_{PTh} (day)	5.0	36.0
τ_{DPo} (day)	15.0	208.0
τ_{PPo} (day)	4.0	93.0
τ_{Pb} (day)	15.0	170.0

much higher ^{234}Th flux was observed in the Hung-Tsai Trough because of the closeness of the sampling site to the landmass. Similarly, the vertical fluxes of ^{210}Po and ^{210}Pb, 400 and 630 dpm m^{-2} d^{-1}, respectively, through the euphotic depth are estimated. It should be noted that the ^{210}Pb flux is about an order of magnitude higher than the atmospheric ^{210}Pb flux of the region. It should also be noted that the vertical ^{210}Pb flux would reduce to 56 dpm m^{-2} d^{-1} if we don't consider horizontal transportation. Whether this reflects the boundary scavenging phenomenon (Bacon et al. 1976) or bias due to an unrealistic scavenging model is unclear and deserves further investigation.

The residence times of the three radionuclides are remarkably comparable to each other. For example, residence times of total ^{234}Th, ^{210}Po, and ^{210}Pb, are 13, 19, and 15 days, respectively. The residence times of the radionuclides would increase from weeks to months if the horizontal transports are neglected. Particle settling velocity, 16 ~ 20 m d^{-1}, obtained by the quotient of the euphoitc depth and $_{PTh}$ or $_{PPo}$, is in a reasonable range for the settling velocity of marine particles.

3.5 Export Fluxes

With the rationale of using ^{234}Th or ^{210}Po as proxies for particulate organic carbon (Murray et al. 2005), export flux in Hung-Tsai Trough is estimated by multiplying the ^{234}Th removal flux to the POC/PTh and by multiplying the ^{210}Po removal flux to the POC/PPo ratio of suspended particles:

$$EP_{Th} = R_{Th} \quad 80 \quad (POC/PTh) \tag{12}$$

$$EP_{Po} = R_{Po} \quad 80 \quad (POC/PPo) \tag{13}$$

The POC/PTh ratio shows its highest value, up to 37 mol dpm^{-1}, in the surface layer of the Hung-Tsai Trough. The ratio decreases dramatically to 2 ~ 6 mol dpm^{-1} in the deep layer. The POC/PTh ratio in the particulate matter of the ocean shows large variability and factors that may attribute to this variability include size, composition, shape, morphology, and the sinking velocity of particles (Bueseller et al. 2006). The organic carbon to ^{210}Po ratio in suspended particles (POC/PPo) ranges from 50 to 300 mol dpm^{-1} with an elevation of the ratio in the mixed and bottom layer. The POC/PPo ratio is 100 ~ 300 mol dpm^{-1} in the mixed layer, which is comparable with the ratio in trap particles collected in the equatorial Pacific (Murray et al. 2005).

The average POC/PTh and POC/PPo of 6 and 150 mol dpm^{-1}, respectively, at the euphotic depth, are used to calculate the export flux from the euphotic layer of the Hung-Tsai Trough. The export flux is 40 mmol m^{-2} d^{-1} estimated from the ^{234}Th flux and 64 mmol m^{-2} d^{-1} estimated from the ^{210}Po flux. Considering the uncertainty of the model, the export fluxes estimated using the two approaches, agree quite well.

The export production deduced from the ^{210}Po-^{210}Pb system is higher than that estimated from the ^{234}Th-^{238}U disequilibria by a factor of 2 (Sarin et al. 1994). Murray et al. (2005) found export based on ^{210}Po is higher than that based on ^{234}Th also by a factor of 2 in the equatorial Pacific. On the contrary, Shimmield et al. (1995) found export production, estimated by the ^{210}Po-^{210}Pb disequilibrium, is an order of magnitude lower than that estimated from the ^{234}Th-^{238}U disequilibrium in the marginal ice zone of Antarctica.

The POC and PN correlate tightly ($n = 30$, $r^2 = 0.96$) and the C/N ratio of suspended particle in the Hung-Tsai Trough is 6.62, identical to the RKR ratio. Accordingly, by multiplying particulate organic carbon flux with the C/N ratio of suspended particles, nitrogen flux via particle settling is 6 ~ 10 mmol N m^{-2} d^{-1} in the Hung-Tsai Trough.

4. CONCLUSIONS

Three stations located at the upper, middle and lower portions of the Hung-Tsai Trough were visited for large-volume seawater sampling. Detailed vertical profiles of dissolved and particulate ^{234}Th, ^{210}Pb, and ^{210}Po were used to compare their geochemical behavior and to estimate export flux in the Hung-Tsai Trough. The findings of this study can be summarized as follows:

(1) ^{234}Th activity is deficient relative to ^{238}U essentially throughout the whole water column. ^{210}Po is also deficient to its secular equilibrium value except in the layer immediately below the mixed layer. ^{210}Pb is in excess of ^{226}Ra activity in the entire water column.

(2) By comparing distribution coefficients of ^{234}Th, ^{210}Pb, and ^{210}Po in the Hung-Tsai Trough, it is found, among the three radionuclides that the ^{210}Po has the highest affinity for particles residing in the surface mixed layer and in the bottom layer.

(3) The DPo/DPb ratio is lower than unity except at some depths in the euphotic zone and in the pycnocline layer, whereas the PPo/PPb ratios are higher than unity only in the surface layer, indicating preferential uptake of ^{210}Po by planktons residing in the surface water and regeneration phenomenon of particles in the intermediate layer of the Hung-Tsai Trough.

(4) The mass balance equations for ^{234}Th, ^{210}Pb, and ^{210}Po need to include horizontal advection to give an accurate estimate of scavenging and removal rates. The scavenging and removal rates for ^{234}Th, ^{210}Pb, and ^{210}Po would be underestimated to give much longer residence times of dissolved and particulate ^{234}Th, ^{210}Pb, and ^{210}Po if horizontal transports were ignored in the Hung-Tsai Trough.

(5) The vertical fluxes of ^{234}Th, ^{210}Pb, and ^{210}Po through the euphotic depth estimated from the scavenging model are 6760, 630, and 400 dpm m^{-2} d^{-1}, respectively. The residence times of the three radionuclides in the euphotic zone are about 2 weeks.

(6) ^{234}Th and ^{210}Po were used as proxies of particulate organic carbon to estimate export flux in the Hung-Tsai Trough. Export flux from the euphotic layer of the Hung-Tsai is 40 mmol C m^{-2} d^{-1} estimated from the ^{234}Th flux and 64 mmol C m^{-2} d^{-1} estimated from the ^{210}Po flux.

Acknoledgements We thank Ms. W. H. Lee for CTD data processing. We appreciate the constructive comments on the manuscript by Dr. S. Luo and an anomalous reviewer. This research was supported through the grant NSC96-2611-M-002-005 from the National Science Council of the Republic of China.

REFERENCES

Anderson, R. F. and A. P. Fleer, 1982: Determination of natural actinides and plutonium in marine particulate material. *Anal. Chem*., **54**, 1142-1147, doi: 10.1021/ac00244a030. [Link]

Bacon, M. P., D. W. Spencer, and P. G. Brewer, 1976: ^{210}Pb/^{226}Ra and ^{210}Po/^{210}Pb disequilibria in seawater and suspended particulate matter. *Earth Planet. Sci. Lett*., **32**, 277-296, doi: 10.1016/0012-821X(76)90068-6. [Link]

Bacon, M. P., R. A. Belastock, R. A. M. Tecotzky, K. K., Turekian, and D. W. Spencer, 1988: Lead-210 and polonium-210 in ocean water profiles of the continental shelf and slope south of New England. *Cont. Shelf Res*., **8**, 841-853, doi: 10.1016/0278-4343(88)90079-9. [Link]

Buesseler, K. O., C. R. Benitez-Nelson, S. B. Moran, A. Burd, M. Charette, J. K. Cochran, L. Coppola, N. S. Fisher, S. W. Fowler, W. D. Gardner, L. D. Guo, O. Gustafsson, C. Lamborg, P. Masque, J. C. Miquel, U. Passow, P. H. Santschi, N. Savoye, G. Stewart, T. Trull, 2006: An assessment of particulate organic carbon to thorium-234 ratios in the ocean and their impact on the application of ^{234}Th as a POC flux proxy. *Mar. Chem*., **100**, 213-233, doi: 10.1016/j.marchem.2005.10.013. [Link]

Chung, Y. and T. Wu, 2005: Large ^{210}Po deficiency in the northern South China Sea. *Cont. Shelf Res*., **25**, 1209-1224, doi: 10.1016/j.csr.2004.12.016. [Link]

Flynn, W. W., 1968: The determination of low levels of polonium-210 in environmental materials. *Analyt. Chim. Acta*., **43**, 221-227, doi: 10.1016/S0003-2670(00)89210-7. [Link]

Harada, K. and S. Tsunogai, 1986: Fluxes of ^{234}Th, ^{210}Po and ^{210}Pb determined by sediment trap experiments in pelagic oceans. *J. Oceanogr. Soc. Jpn*., **42**, 192-200, doi: 10.1007/BF02109353. [Link]

Honeyman, B. D., L. S. Balistrieri, and J. W. Murray, 1988: Oceanic trace metal scavenging: The importance of particle concentration. *Deep-Sea Res*., **35**, 227-246, doi: 10.1016/0198-0149(88)90038-6. [Link]

Hung, C. C. and C. L. Wei, 1992: Th-234 scavenging in the water column off southwestern Taiwan. *Terr. Atmos. Ocean. Sci*., **3**, 183-197.

Kim, G. and T. M. Church, 2001: Seasonal biogeochemical fluxes of ^{234}Th and ^{210}Po in the upper Sargasso Sea: Influence from atmospheric iron deposition. *Global Biogeochem. Cycles*, **15**, 651-661, doi: 10.1029/2000GB001313. [Link]

Ku, T. L., K. G. Knauss, and G. G. Mathiew, 1977: Uranium in open ocean: Concentration and isotopic composition. *Deep-Sea Res*., **24**, 1005-1017, doi: 10.1016/0146-6291(77)90571-9. [Link]

Ku, T. L., S. Luo, M. Kusakabe, and J. K. B. Bishop, 1995: ^{228}Ra-derived nutrient budgets in the upper equatorial Pacific and the role of "new" silicate in limiting productivity. *Deep-Sea Res. II*, **42**, 479-497, doi: 10.1016/0967-0645(95)00020-Q. [Link]

Liang, N. K., J. G. Chang, C. H. Su, and K. I. Wang, 1985: Data report of temperature and current measurement in the Hung-Tsai Trough off southern Taiwan, Special Report # 19, Institute of Habor and Marine Technology, Taiwan, 122 pp.

Liang, W. D., T. Y. Tang, Y. J. Yang, M. T. Ko, and W. S. Chuang, 2003: Upper-ocean currents around Taiwan. *Deep-Sea Res. II*, **50**, 1085-1105, doi: 10.1016/S0967-0645(03)00011-0. [Link]

Murray, J. W., B. Paul, J. P. Dunne, and T. Chapin, 2005: ^{234}Th, ^{210}Pb, ^{210}Po and stable Pb in the central equatiorial Pacific: Tracers for particle cycling. *Deep-Sea Res. I*, **52**, 2109-2139, doi: 10.1016/j.dsr.2005.06.016. [Link]

Nozaki, Y., N. Ikuta, and M. Yashima, 1990: Unusually large ^{210}Po deficiencies relative to ^{210}Pb in the Kuroshio Current of the East China and Philippine seas. *J. Geophys. Res*., **95**, 5321-5329, doi: 10.1029/JC095iC04p05321. [Link]

Nozaki, Y., V. Kasemsupaya, and H. Tsubota, 1990: The distribution of ^{228}Ra and ^{226}Ra in the surface waters of the northern North Pacific. *Geochem. J*., **24**, 1-6.

Nozaki, Y., F. Dobashi, Y. Kato, and Y. Yamamoto, 1998: Distribution of Ra isotopes and the ^{210}Pb and ^{210}Po balance in surface seawaters of the mid Northern Hemisphere. *Deep-Sea Res. I*, **45**, 1263-1284, doi: 10.1016/S0967-0637(98)00016-8. [Link]

Nozaki, Y. and Y. Yamamoto, 2001: Radium 228 based nitrate fluxes in the eastern Indian Ocean and the South China Sea and a silicon-induced "alkalinity pump" hypothesis. *Global Biogeochem. Cycles*, **15**, 555-567, doi: 10.1029/2000GB001309. [Link]

Sarin, M. M., S. Krishnaswami, R. Ramesh, and B. L. K. Somayalulu, 1994: ^{238}U decay series nuclides in the northeastern Arabian Sea: Scavenging rates and cycling processes. *Cont. Shelf Res*., **14**, 251-265, doi: 10.1016/0278-4343(94)90015-9. [Link]

Sarin, M. M., G. Kim, and T. M. Church, 1999: ^{210}Po and ^{210}Pb in the south-equatorial Atlantic: Distribution and disequilibrium in the upper 500 m. *Deep-Sea Res. II*, **46**, 907-917, doi: 10.1016/S0967-0645(99)00008-9. [Link]

Savoye, N., C. Benitez-Nelson, A. B. Burd, J. K. Cochran, M. Charette, K. O. Buesseler, G. A. Jackson, M. Roy-Barman, S. Schmidt, and M. Elskens, 2006: ^{234}Th sorption and export models in the water column: A review. *Mar. Chem*., **100**, 234-249, doi: 10.1016/j.marchem.2005.10.014. [Link]

Shannon, L. V., R. D. Cherry, and M. J. Orren, 1970: Polonium-210 and lead-210 in the marine environment. *Geochim. Cosmochim. Acta*, **34**, 701-711, doi: 10.1016/0016-7037(70)90072-4. [Link]

Shaw, P. T., 1989: The intrusion of water masses into the sea southwest of Taiwan. *J. Geophys. Res*., **94**, 18213-18226, doi: 10.1029/JC094iC12p18213. [Link]

Shimmield, G. B., G. D. Ritchie, and T. W. Fileman, 1995: The impact of marginal ice zone processes on the distribution of ^{210}Pb, ^{210}Po and ^{234}Th and implications for new production in the Bellingshausen Sea, Antarctica. *Deep-Sea Res. II*, **42**, 1313-1335, doi: 10.1016/0967-0645(95)00071-W. [Link]

Tanaka, N. and S. Tsunogai, 1983: Behavior of ^{7}Be in Funka Bay, Japan, with reference to those of insoluble nuclides, ^{234}Th, ^{210}Po and ^{210}Pb. *Geochem. J.*, **17**, 9-17.

Wei, C. L. and J. W. Murray, 1991: ^{234}Th/^{238}U disequilibria in the Black Sea. *Deep-Sea Res.*, **38**, s855-s873.

Wei, C. L. and J. W. Murray, 1994: The behavior of scavenged isotopes in marine anoxic environments: ^{210}Pb and ^{210}Po in the water column of the Black Sea. *Geochim. Cosmochim. Acta*, **58**, 1795-1811, doi: 10.1016/0016-7037(94)90537-1. [Link]

Wei, C. L., K. L. Jen, and K. Chu, 1994: Sediment trap experiments in the water column off southwestern Taiwan: ^{234}Th fluxes. *J. Oceanogr.*, **50**, 403-414, doi: 10.1007/BF02234963. [Link]

Yang, M. D., 2001: Atmospheric ^{210}Pb fluxes in metropolitan Taipei, Taiwan. Master Thesis, National Taiwan University, Taipei, Taiwan, ROC, 108 pp.

Yu, H. S. and C. S. Chiang, 1995: Morphology and origin of the Hongtsai submarine canyon west of the Hengchun Peninsula, Taiwan. *J. Geol. Soc. China*, **38**, 81-93.